Multiple Conformations of NAD and NADH When Bound to Human Cytosolic and Mitochondrial Aldehyde Dehydrogenase†

Philip K. Hammen,*,‡ Abdellah Allali-Hassani,‡ Klaas Hallenga,§ Thomas D. Hurley,⊥ and Henry Weiner‡,||

Department of Biochemistry, Purdue University, 1153 Biochemisty Building, West Layfayette, Indiana 47907-1153, Department of Biochemistry, Purdue University, West Lafayette, Indiana 47907-1153, Department of Chemistry, Purdue University, West Lafayette, Indiana 47907, and Department of Biochemistry and Molecular Biology, Indiana University School of Medicine, Indianapolis, Indiana 46202

Received December 27, 2001; Revised Manuscript Received March 25, 2002

ABSTRACT: Crystallographic analysis revealed that the nicotinamide ring of NAD can bind with multiconformations to aldehyde dehydrogenase (ALDH) (Ni, L., Zhou, J., Hurley, T. D., and Weiner, H. (1999) *Protein Sci. 8*, 2784−2790). Electron densities can be defined for two conformations, neither of which appears to be compatible with the catalytic reaction. In one conformation, it would prevent glutamate 268 from functioning as a general base needed to activate the catalytic nucleophile, cysteine 302. In the other confromation, the nicotinamide is too far from the enzyme−substrate adduct for efficient hydride transfer. In this study, NMR and fluorescence spectroscopies were used to demonstrate that NAD and NADH bind to human liver cytosol and mitochondrial ALDH such that the nicotinamide samples a population of conformations while the adenosine region remains relatively immobile. Although the nicotinamide possesses extensive conformational heterogeneity, the catalyzed reaction leads to the stereospecific transfer of hydride to the coenzyme. Mobility allows the nicotinamide to move into position to be reduced by the enzyme−substrate adduct. Although the reduced nicotinamide ring retains mobility after NADH formation, the extent of the motion is less than that of NAD. It appears that after reduction the population of favored nicotinamide conformations shifts toward those that do not interfere with the ability of the enzyme to release the reaction product. In the case of the mitochondrial, but not the cytosolic, enzyme this change in conformational preference is promoted by the presence of Mg^{2+} ions. Coenzyme conformational mobility appears to be beneficial to catalysis by ALDH throughout the catalytic cycle.

Structures of three different mammalian liver aldehyde dehydrogenase (ALDH)[1] isozymes have been reported in the literature (*1*−*3*). One of the features of these structures that distinguish them from other dehydrogenases is in the binding region of the coenzyme. Like other NAD binding proteins, ALDH utilizes a Rossmann fold for its interaction with the coenzyme. However, the Rossmann fold in ALDH is a variant of the typical structure with unique features that have been described in detail (*1*). One consequence of the difference in structure is that the enzyme makes fewer contacts with the coenzyme upon binding. Other dehydrogenases typically have a residue with a positively charged side chain near the phosphodiester region of the coenzyme (*2*). In addition, the dipole of α-helix A of the Rossmann fold is typically oriented toward the phosphates of NAD. In each of the mammalian structures, ALDH lacks a residue that could bind the negatively charged phosphodiester group through an ionic interaction. The phosphodiester group is more distant from helix A than it is in other dehydrogenases (*1*).

Electron density corresponding to the nicotinamide portion of the coenzyme was not found in the bovine ALDH2 crystal containing 0.2 mM $MgCl_2$ (*2*). Substitution of 2 mM $SmCl_3$ for $MgCl_2$ gave data in which all of the coenzyme was observed. However, when the entire NAD molecule was observed in ALDH1 and ALDH2, it appeared to have more than one favored conformation (*2*, *3*). The principal differences were seen in the phosphodiester linking the nucleotides, leading to two different sets of coordinates for the nicotinamide end of the coenzyme molecule. The NAD structures are shown in Figure 1 with the adenine rings oriented identically. In sheep ALDH1, the nicotinamide ring adopted a contracted position with a distance of 11.2 Å from the center of the adenine ring to that of the nicotinamide ring. In this structure, the nicotinamide is more than 6 Å from C302, the residue that covalently binds the aldehyde substrate (*4*), and appears to be too far away for efficient hydride transfer (*3*). In the ALDH2 structure, the nicotinamide is more extended with a distance of 13.3 Å from the center of the adenine ring to that of the nicotinamide ring. In this case, the position of the coenzyme is sufficiently close to allow

† This work was supported by a grant from the National Institutes of Health, AA05812, to H.W., and AA11982, to T.D.H. This is paper number 16784 from the Purdue Agriculture Experiment Station.

* Corresponding author. Phone: (765) 494-7672. Fax: (765) 494-7897. E-mail: hammen@purdue.edu.

‡ Department of Biochemistry, Purdue University.

§ Department of Chemistry, Purdue University.

⊥ Indiana University School of Medicine.

|| Submitting author: Dr. Henry Weiner. Phone: (765) 494-1650. Fax: (765) 494-7897. E-mail: hweiner@purdue.edu.

[1] Abbreviations: ALDH1, human liver cytosol aldehyde dehydrogenase; ALDH2, human liver mitochondrial aldehyde dehydrogenase; STD, saturation transfer difference NMR; FRET, fluorescence resonance energy transfer; TrNOESY, two-dimensional transferred nuclear Overhauser enhancement spectroscopy.

10.1021/bi012197t CCC: $22.00
Published on Web 05/10/2002

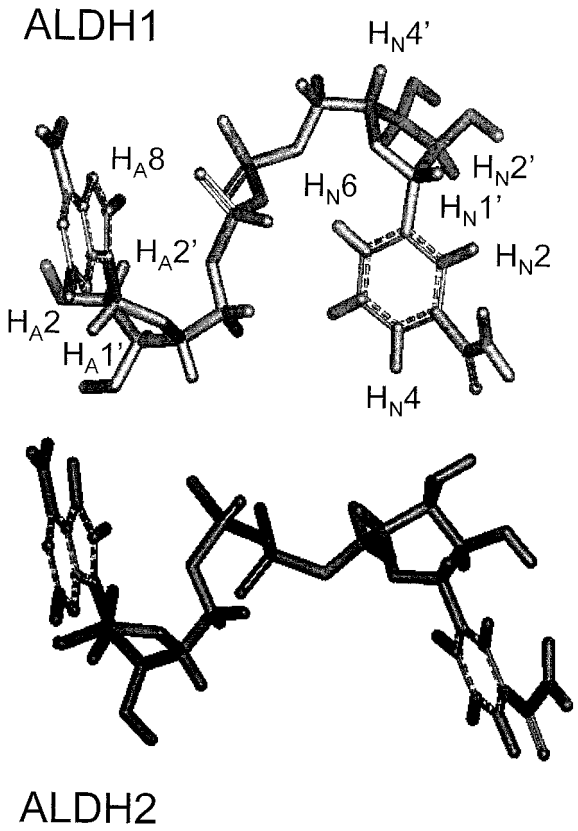

FIGURE 1: Comparison of NAD structures while bound to ALDH1 (top) and ALDH2. Adenine rings of the two structures were aligned for purposes of comparison.

hydride transfer, but the nicotinamide ring obstructs the abstraction of a proton from C302 by the general base, E268 (*5*). The structures show two different coenzyme conformations, both of which appear to leave the nicotinamide ring out of position to participate efficiently in catalysis.

The available structural data are not helpful in answering questions about how the coenzyme participates in catalysis by ALDH. It is not known whether NAD can move freely when bound to ALDH or the enzyme binds NAD in two different conformations that cannot interconvert without dissociating. Similarly, it is not known whether the conformational heterogeneity of the coenzyme observed in the crystal structure can afford ALDH an enzymatic advantage. From a thermodynamic perspective, coenzyme binding should be entropically favorable when a portion of the bound molecule can move freely. Previous studies with ALDH point mutants have shown that most mutation effects are on coenzyme binding (*6*). As yet, there are no structural data pertaining to the reduced coenzyme when bound to ALDH. In addition, Mg^{2+} ions have been shown to stimulate the activity of ALDH2 but impair the activity of ALDH1 (*7*). In this study, we employ solution spectroscopic methods to develop a better understanding of how coenzyme binding is involved in the catalysis of ALDH1 and ALDH2.

EXPERIMENTAL PROCEDURES

Materials. NAD and NADH were purchased from Sigma; Sequenase version 2.0 kit was obtained from United States Biochemical Corp.; Minipreps DNA purification kit was purchased from Biolabs and T4 DNA ligase was purchased from Promega Corp.; GeneClean kit was purchased from Bio 101, Inc.; [^{35}S]dATP was purchased from Amersham Corp.; and the restriction enzymes used were purchased from either New England Biolabs or Promega Corp. Acetaldehyde-d_4 was purchased from Aldrich. Deuterium oxide was purchased from Cambridge Isotope Labs.

Cells and Plasmids. Native or mutant ALDH1 and ALDH2 cDNAs were cloned into the pT7−7 expression vector, and expressed in the *Escherichia coli* strain BL21 (DE3) pLysS (*8*) as reported previously (*6*, *9*). To construct human ALDH mutants, the oligonucleotide primers containing the mutation were used for site-directed mutagenesis with the Mutagene Kit (Bio-Rad), following the manufacturer's instructions. The mutant colonies were selected by a sequencing method that employed dideoxynucleotide chain-termination (*10*). After mutant colonies were identified, the cDNA fragment containing the mutant was exchanged with the corresponding fragment of the native ALDH cDNA from the pT7−7 plasmid. They were transformed in BL21 (DE3) pLysS cells possessing the chloramphenicol resistance pLysS plasmid. The mutation was again confirmed by double-stranded DNA sequencing of the pT7−7 plasmid.

Expression of ALDH1 and ALDH2. The enzymes were expressed and purified as described previously (*5*, *6*). Important details of the procedure are that recombinantly expressed enzymes were treated with protamine sulfate (1.25 mg/mL) followed by anion exchange (DEAE−cellulose) and 4-hydroxyacetophenone-based affinity chromatography (*11*). The purity of the enzymes was determined to be >95% by SDS−PAGE using the Coomassie Blue staining procedure. Fractions containing only ALDH activity were pooled and concentrated using a Centricon centrifugal protein concentration device (Amicon). While not in use, purified enzyme was stored at −20 °C in a 50% glycerol solution.

NMR Spectroscopy. Purified protein was dialyzed into phosphate-buffered ^2H_2O (50 mM sodium phosphate, pH 7.4). The final protein concentration was ca. 35 μM. To determine the appropriate concentrations of coenzyme for the TrNOESY experiments (*12*), aliquots of NAD were added to a solution of 35 μM ALDH so the concentration increased in 1 mM increments. A final concentration of 3−4 mM was determined to be optimal. Subsequently, the dialyzed protein solution was used to dissolve 1.2 mg of lyophilized coenzyme. Because ALDH1 and ALDH2 are tetrameric enzymes, the nominal ratio of ligand to active sites was 25:1. A series of TrNOESY spectra were obtained with mixing times of 20, 60, 100, 150, 200, and, in some cases, 250 ms at 20 °C. A Varian UNITYplus 600 MHz NMR spectrometer was used. Two-dimensional (2D) transformation included the subtraction of low-frequency signal associated with residual solvent. All chemical shifts were referred to a residual ^1H_2O signal at 4.8 ppm. After transformation, cross peak volumes were measured by either volume integration or from the number of contours. Fractional cross peak volumes were calculated by dividing the cross peak volume by the auto-peak volume obtained from the 20 ms data. Processing software was NT-NMRPipe (*13*) or VNMR (Varian Associates, Inc.).

To determine the stereospecificity of hydride transfer, a 0.1 mL portion of a NMR sample previously described was diluted to 0.5 mL with phosphate-buffered ^2H_2O (pH 7.4) containing 1.2 mg of NAD and 15 μL of acetaldehyde-d_4. After 30 min and 2 h, NMR spectra were obtained to observe

the pattern of deuterium labeling in the NADH that had been formed in situ.

The samples used for TrNOESY experiments were also used for STD experiments. For the STD experiments, selective saturation pulses were not required. The technique relied upon frequency and power switching of the radio frequency transmitter. The transmitter was moved to the edge of the spectrum and used at low power to achieve saturation with times of 0.2, 0.3, 0.4, 0.6, 0.8, and 1.0 s. The on-resonance frequency was positioned 4000 Hz to the high-field side of the water resonance (i.e., −2 ppm). The off-resonance frequency was placed 50 000 Hz to the low-field side of the water resonance. After saturation, the transmitter was placed at the water frequency and a hard 90° pulse was used, followed by a spin−echo pulse train that refocused magnetization prior to spectral acquisition.

Fluorescence Spectroscopy. Fluorescence spectra were acquired using a J.Y. Horiba Fluorolog-3 spectrofluorometer at 20 °C. Protein concentrations were limited to 1 μM to keep absorption at 278 nm below 0.05, thereby avoiding inner-filter effects in the emission. For FRET spectra, excitation was set to 290 nm and emission was scanned from 310 to 500 nm. Energy-transfer efficiencies (E) were estimated with the use of the equation

$$E = (F_D - F_{DA})/F_D$$

in which F_D and F_{DA} are the tryptophan fluorescence intensities in the absence and presence of the NADH acceptor, respectively (*14*, *15*). Structural data (*2*, *3*) show that each isozyme possesses two tryptophan side chains located within 10 Å of the center of the nicotinamide ring. Therefore, it was not possible to know reliably which of the possible donors had the greatest influence on the spectrum. Fluorescence anisotropy of NADH was measured with excitation wavelength of 350 nm and an emission wavelength of 450 nm. These wavelengths displayed the maximum response when excitation and emission spectra were obtained with polarization. A total of 10 measurements were obtained for each sample.

Structure Analyses. Coenzyme structures were obtained from the sheep ALDH1 (1bxs) and human ALDH2 (1cw3) structures that have been deposited in the Brookhaven Protein Structure Data Bank. The structures were loaded into QUANTA98, version 98.1111 (Molecular Simulations, Inc.). The "A" subunit was used for all structure modeling work. Hydrogen atoms were added to the coenzyme molecule using standard routines of the software package.

RESULTS

Conformational Heterogeneity of NAD and NADH When Bound to ALDH

The initial question regarding coenzyme conformation had to do with the nature of the multiple NAD conformations observed in the crystal structure. Both NMR and fluorescence techniques were used to assess coenzyme conformational mobility and contact with the enzyme.

Saturation Transfer. One method of using NMR to observe structural characteristics of the coenzyme while bound to ALDH1 and ALDH2 was with STD experiments. This technique utilizes the spin diffusion of the protein to transfer a state of saturation to the bound ligand (*16*, *17*). In this method, radio frequency irradiation is applied to the broad protein resonances located at the edge of the spectrum (e.g., −2 ppm), far from the ligand resonances. For a large protein such as ALDH, efficient spin diffusion rapidly produces a state of saturation throughout the protein without affecting free ligand molecules. Bound ligand protons that are spatially near to saturated protein protons will also become saturated via intermolecular cross relaxation. The extent of saturation that is transferred to specific protons of the ligand depends on several factors. The phenomenon depends on the presence of nearby transfer partners in the protein. Rates of spin diffusion within the protein and from the protein to the ligand will increase with the rotational correlation time of the protons. Other factors that may affect saturation transfer are T_1 relaxation and the kinetics of the protein−ligand interaction.

STD experiments were performed on mixtures of NAD with ALDH1 or ALDH2. A clear difference was observed in the amount of saturation transferred to protons of the adenine ring when compared to protons of the nicotinamide ring (Figure 2A). Of the protons resolved in the spectrum, the greatest amount of saturation was obtained by H_A2, followed by H_A1' and H_A8. Protons associated with the nicotinamide, H_N2, H_N4, H_N5, H_N6, and H_N1', all showed a similar extent of saturation transfer which was 2−3 times less than that observed with H_A8 or H_A1' (Figure 2B). One interpretation of these data is that NAD adopts a single conformation when it binds and that the adenosine portion is more intimately associated with the enzyme than the nicotinamide portion. An alternative explanation of the disparity between adenine and nicotinamide rings is that the adenine is bound in a relatively fixed position while the nicotinamide can move more freely.

The varying intensities of saturation transfer among protons of the adenine reflect their distances from non-exchangeable protons of the protein. The uniformity of intensities observed for the nicotinamide protons is consistent with an averaging phenomenon in the extent of saturation transfer. To assess the relative differences of saturation transfer in the adenine and nicotinamide segments, ratios of saturation transfer intensities were computed for various pairs of protons. When computed, the ratios were independent of the saturation times that were employed, so the values obtained for a series could be averaged (Figure 3). The ratios provide a means of monitoring the variation of response from protons of the nicotinamide relative to those of the adenine ring. It can be seen from the figure that the adenine protons are saturated to a greater extent than those of the nicotinamide and that, for each enzyme, the nicotinamide protons are saturated uniformly.

The ALDH crystallographic data show that the Glu399 side chain appears to be involved in hydrogen bonds with the C2′ and C3′ hydroxyl groups of the nicotinamide ribose in NAD (*2*). For both ALDH1 (Hassani and Weiner, unpublished observations) and ALDH2 (*18*), an E399Q mutation resulted in the change of rate-determining step to hydride transfer, the step in which NADH is formed. This change in kinetics suggests that, in the mutant, the nicotinamide ring is not as available to accept the hydride as it is in the native protein. When the saturation transfer experiment was performed on a mixture of E399Q and NAD, the

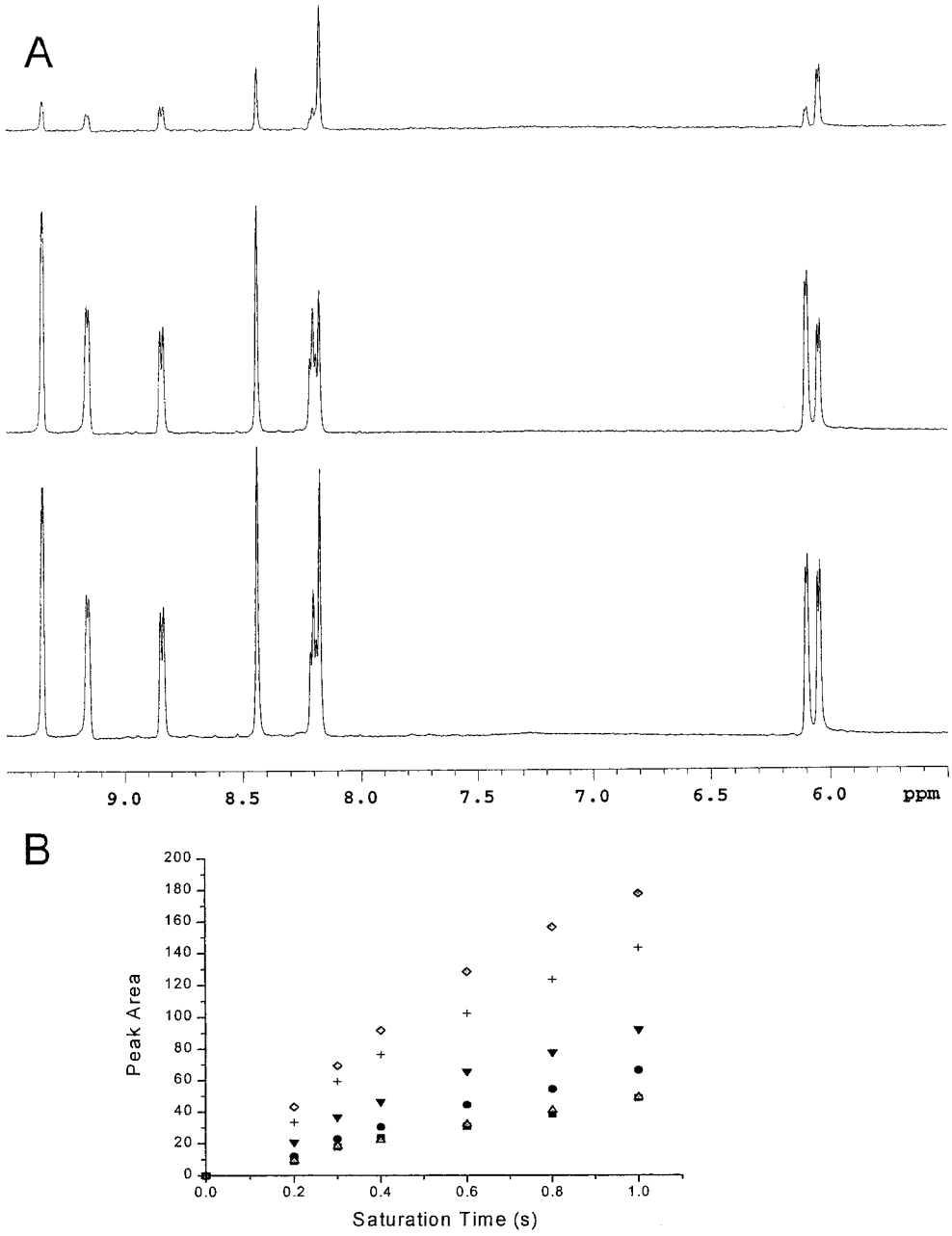

FIGURE 2: (A) NMR spectra from the STD experiment involving ALDH2 and NAD. Saturation time was 1.0 s. Chemical shift assignments are H_N2 (9.36), H_N6 (9.13), H_N4 (8.82), H_A8 (8.42), H_N5 (8.20), H_A2 (8.18), H_N1' (6.12), and H_A1' (6.03). The bottom spectrum is the control, with saturation off-resonance. The middle spectrum is the experiment, with saturation at ca. −2 ppm. The difference is shown at the top. (B) Increase of saturation transfer for various NAD protons as a function of saturation time. Protons plotted are as follows: (■) H_N2, (●) H_N4, (▼) H_A8, (◇) H_A2, (△) H_N1', and (+) H_A1'. Values on the *y* axis are integrated peak areas obtained from difference spectra.

disparity of saturation transfer increased between adenine and nicotinamide protons (Figure 3A). The extent of increase ranged from ca. 10% in the H_A8/H_N2 comparison to nearly 100% in the comparison of H_A1' and H_N1'. The E399Q mutation eliminated an important charge−dipole interaction between ALDH and NAD. There are two possible explanations for the STD observations. One is an increase in conformational mobility of the nicotinamide and the second is that NAD bound to the mutant in a single, static conformation in which the nicotinamide protons were more distant from any protons of the protein.

The STD experiments were performed with the two ALDH isozymes and NADH. When NADH was the ligand, the disparity in saturation transfer between the adenine and nicotinamide ends of the molecule was reduced by ca. 50% (Figure 4A). In this case, the saturation attained by nicotinamide protons and H_A8 were nearly equivalent (i.e., with ratios approaching one).

The addition of magnesium ions to the samples containing NAD produced similar responses in ALDH1 and ALDH2. Saturation transfer actually decreased in magnitude as magnesium concentration increased. However, the adenine/nicotinamide ratios remained virtually constant at 0, 2, and 10 mM Mg^{2+} ions (Figure 3A−C). When Mg^{2+} ions were added to the E399Q/NAD mixture, the adenine/nicotinamide ratios, and thus conformational mobility, became similar to that of the native enzymes (Figure 3A−C). When the ligand was NADH, the change in adenine/nicotinamide ratios for ALDH1 and ALDH2 differed (Figure 4A−C). With ALDH1, the ratios H_A8/H_N2, H_A8/H_N2', H_A1'/H_N2, and H_N1'/H_N2' all

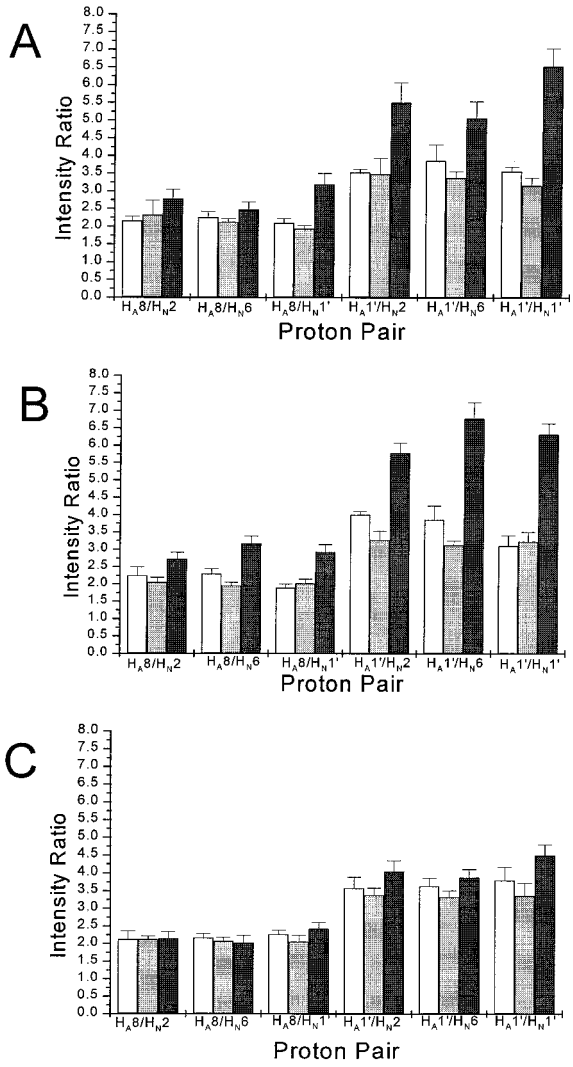

FIGURE 3: Saturation transfer ratios of adenosine protons to nicotinamide protons of NAD when bound to ALDH1 (left), ALDH2 (middle), and the ALDH1 E399Q mutant (right) with Mg^{2+} ion concentrations of (A) 0 mM, (B) 2 mM, and (C) 10 mM. On-resonance spectra were subtracted from off-resonance for experiments with saturation times of 0.2, 0.3, 0.4, 0.6, 0.8, 1.0, and 1.2 s. Peaks in the difference spectra were integrated to obtain areas. Ratios were calculated for each saturation time, and all the ratios were averaged to obtain the values that were plotted.

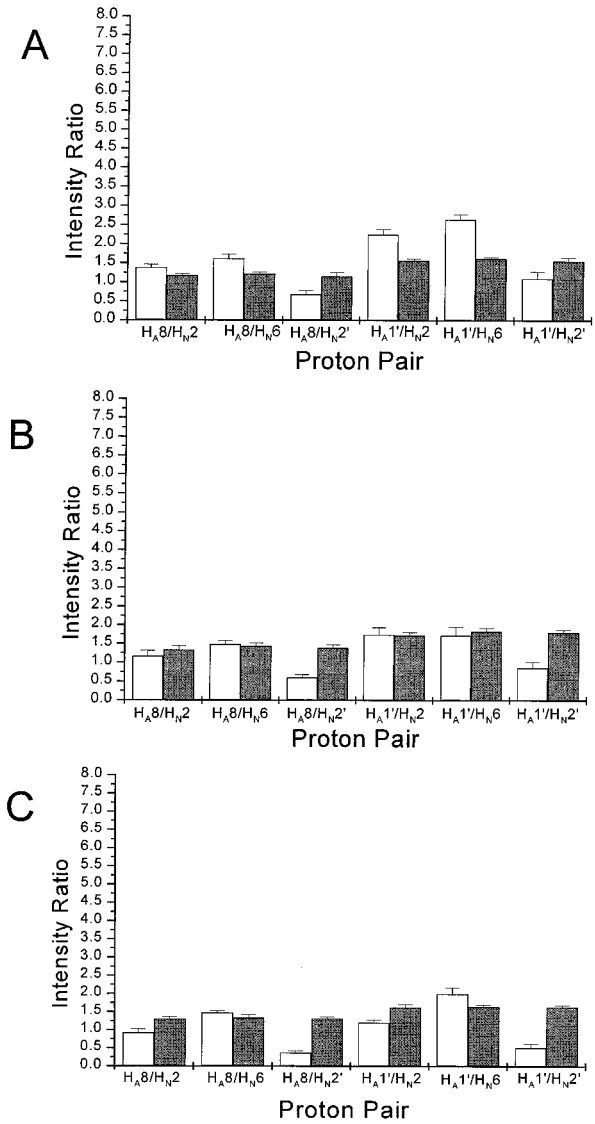

FIGURE 4: Saturation transfer ratios of adenosine protons to nicotinamide protons of NADH when bound to ALDH1 (left) and ALDH2 (right) with Mg^{2+} ion concentrations of (A) 0 mM, (B) 2 mM, and (C) 10 mM. On-resonance spectra were subtracted from off-resonance for experiments with saturation times of 0.2, 0.3, 0.4, 0.6, 0.8, 1.0, and 1.2 s. Peaks in the difference spectra were integrated to obtain areas. Ratios were calculated for each saturation time, and all the ratios were averaged to obtain the values that were plotted.

decreased in magnitude as $[Mg^{2+}]$ increased. The data showed that the nicotinamide proton interactions with ALDH1 were increasing relative to adenine with increasing Mg^{2+} ion concentration. For NADH bound to ALDH2, these ratios were independent of Mg^{2+} ion concentration.

A clear difference between ALDH1 and ALDH2 could be seen in the relative amount of saturation accumulated by H_N2' in the presence of Mg^{2+} ions. Without Mg^{2+} ions, when NADH was bound to either ALDH1 or ALDH2, H_N2' became saturated to a similar extent as H_A8 or H_A1'. A difference between the isozymes became apparent with the addition of Mg^{2+} ions, as H_N2' became more saturated than the adenine protons upon interaction with ALDH1. With ALDH2, H_N2' saturation was essentially independent of cation concentration. The data indicate a variation in the exposure of H_N2' to the coenzyme binding region of the two enzymes.

Fluorescence Anisotropy. A ligand that retains mobility while bound to an enzyme should display anisotropic motion relative to the enzyme. Because of its fluorescence properties, NADH can be observed while interacting with ALDH. To obtain information about NADH motion when bound to ALDH, fluorescence anisotropy studies were undertaken. Data were obtained for an ALDH−NADH complex alone and after the addition of Mg^{2+} ions. The anisotropy of NADH free in phosphate buffer was ca. 0.01. It was 0.15 when combined with ALDH1 and 0.10 with ALDH2. In the case of both isozymes, the anisotropy increased as Mg^{2+} ions were added, reaching a value of ca. 0.25 in the presence of 10 mM Mg^{2+} ions (Figure 5). These data can be interpreted to indicate that, although bound to the enzyme, NADH maintained significant mobility, which was more restricted in the presence of Mg^{2+} ions. Subsequent addition of the substrate, propanal, produced no further change in anisotropy (Figure 5). These data provide an indication that the substrate does

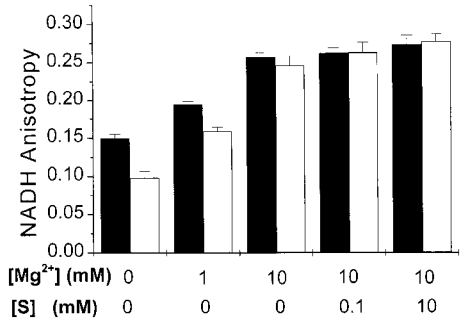

FIGURE 5: Affect of Mg^{2+} ions and the substrate propanal (S) on fluorescence anisotropy of NADH at 20 °C while bound to ALDH1 (black) and ALDH2 (white). The concentration of protein in the samples was 1 μM and the NADH concentration was 1 μM. A total of 10 measurements were made for each condition with excitation at 350 nm and emission at 450 nm. Error bars represent the standard error of the 10 measurements.

not play the role of restricting the coenzyme to a single, productive conformation.

Fluorescence Resonance Energy Transfer. Fluorescence data was obtained to observe changes in the environment of the NADH nicotinamide ring while bound to ALDH. Excitation of the seven tryptophan residues in ALDH at 290 nm resulted in a fluorescence envelope with a maximum at ca. 350 nm. When NADH was added, tryptophan fluorescence decreased by 5−6%, suggesting a potential energy-transfer mechanism for the quenching of fluorescence. The addition of Mg^{2+} ions resulted in further quenching of tryptophan fluorescence and a visible increase in emission with a maximum at 435 nm representing NADH fluorescence (Figure 6). Each enzyme displayed similar FRET behavior upon the addition of increasing amounts of Mg^{2+} ion (Table 1). After the addition of 10 mM Mg^{2+} ions, total energy-transfer efficiency was 0.38 for ALDH1 and 0.34 for ALDH2. These data suggest the interpretation that the addition of Mg^{2+} ions results in a change in the orientation of the nicotinamide ring relative to tryptophan side chains of the proteins.

Stereospecificity of Hydride Transfer

Because NAD appears to bind to ALDH with a high degree of conformational heterogeneity, it is possible that the nicotinamide could rotate freely about the glycosidic bond. Complete rotation would produce interconversion between the syn and anti conformers. In this case, hydride transfer would not be stereospecific. It was previously shown that hydride transfer is stereospecific in the reaction catalyzed by the dimeric isozyme, ALDH3 (*19*).

Experiments were carried out with ALDH1 and ALDH2 to determine if the reaction was stereospecific with these enzymes. Acetaldehyde-d_4 was added to a NMR sample containing an ALDH isozyme and NAD to observe the presence or absence of signals in the NADH that was produced. The NADH spectrum normally contains resonances for the H_N4 protons at 2.85 and 2.72 ppm. NMR spectra were acquired 0.5 and 2 h after the samples were mixed. In the experiments with both ALDH1 and ALDH2, only the resonance at 2.72 ppm appeared. The deuterium had been incorporated stereospecifically in place of the proton at 2.85 ppm. Therefore, both ALDH1 and ALDH2 possess A-side (pro-R) specificity, as did ALDH3. Although the nicotinamide is mobile, the mobility does not appear to include complete rotation about the glycosidic bond.

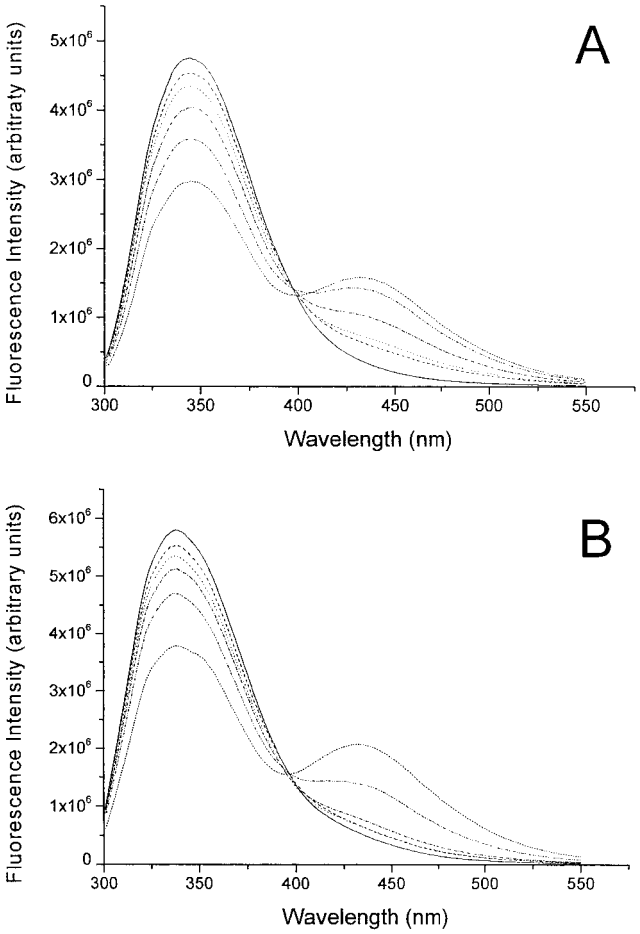

FIGURE 6: Fluorescence resonance energy-transfer phenomena observed for the binding of NADH (1 μM) to 1 μM ALDH1 (A) and ALDH2 (B) at 20 °C. Excitation was set to 290 nm and emission was scanned from 310 to 500 nm. Aliquots of $MgCl_2$ were added so the affect of Mg^{2+} ions on the spectra could be observed. The spectra in the figure (from top to bottom at 350 nm) have Mg^{2+} ion concentrations of 0, 1 μM, 10 μM, 100 μM, 1 mM, and 10 mM.

Table 1: Quenching of ALDH Fluorescence by Energy Transfer to NADH

	ALDH1		E399Q[a]		ALDH2	
solution	Fl int[b]	E[c]	Fl int	E	Fl int	E
enzyme only (F_D)	4.8	0	5.3	0	5.8	0
+1 μM NADH	4.5	0.06	5.3	0	5.5	0.05
+10 μM Mg^{2+}	4.3	0.10	5.1	0.04	5.4	0.07
+100 μM Mg^{2+}	4.0	0.17	4.8	0.09	5.1	0.12
+1 mM Mg^{2+}	3.6	0.25	4.3	0.19	4.7	0.19
+10 mM Mg^{2+}	3.0	0.38	4.0	0.25	3.8	0.34

[a] Mutant of ALDH1. [b] Fluorescence intensity ($\times 10^{-6}$) after blank correction. [c] Energy-transfer efficiencies, E, calculated using the equation, $E = (F_D - F_{DA}/F_D)$. Fluorescence values are F_D for donor and F_{DA} for donor in the presence of the acceptor, NADH.

TrNOESY Studies of Coenzyme Conformational Preference

Distances between hydrogen atoms in the two NAD structures were determined from the structural models. The values for critical hydrogen pairs are displayed in Table 2. Distances in the adenosine portion are very similar for

Table 2: Selected Interproton Distances (Å) in Hydrogen-Containing NAD Models Generated from the Structures of ALDH1 and ALDH2 in Complex with NAD

proton pair	ALDH1	ALDH2
HN2−HN1′	2.32	2.22
HN6−HN1′	3.76	3.66
HN2−HN2′	3.39	4.32
HN2−HN3′	5.06	5.70
HN6−HN2′	3.81	2.12
HN6−HN3′	2.92	4.30
HA8−HA1′	3.80	3.87
HA8−HA2′	2.18	1.99
HA1′−HA2′	3.00	3.07
HA2−HA1′	4.84	4.70

ALDH1 and ALDH2. Distances relating the protons of the nicotinamide ring and ribose protons H_N2' and H_N3' display dramatic differences. These distances reveal that the conformations differ not only in the phosphodiester linkage but also in the local conformation of the nicotinamide. If bound NAD is in a state of high conformational mobility, the sources of that motion could arise from both the phosphodiester portion of the molecule and from rotation of the nicotinamide ring.

Theoretical NOESY spectra for the NAD conformation found in both ALDH1 and ALDH2 structures would be expected to have a large H_N2-H_N1' cross peak and a much smaller H_N6-H_N1' cross peak. The principle difference would be that the NAD conformation of the ALDH1 structure would generate a larger interaction for H_N6-H_N3' than for H_N6-H_N2'. In stark contrast, the NAD conformation of the ALDH2 structure would feature an extremely large H_N6-H_N2' interaction and virtually nothing from the interaction of H_N6 with H_N3'. In the absence of NAD conformation averaging, the two conformations could be readily distinguished with NMR spectra.

Conformational Preferences of NAD When Bound to ALDH. To investigate the conformational preferences of NAD when bound to each isozyme, a series of transferred-NOESY spectra were obtained using both ALDH1 and ALDH2 with NAD at 20 °C. At the adenosine end of NAD, the H_A8-H_A1' interaction appeared throughout the data set while the H_A2-H_A1' interaction was observed only at $\tau_m >$ 100 ms (Figure 7). This relationship is consistent with the anti conformation, which is common for NAD molecules bound to dehydrogenases (*20*−*22*) and is consistent with the crystallographic data (Table 2). However, the crystal structures predict an even larger interaction between the H_A8-H_A2' pair. Data corresponding to H_A2' were attenuated because the chemical shift of this proton was coincident with that of the solvent. Data collection or data processing techniques designed to remove the solvent signal also resulted in the attenuation of data for H_A2'. Therefore, it was not possible to assess the relative magnitude of the H_A8-H_A2' cross peak.

Cross peaks involving nicotinamide protons differed from predictions of the crystal structure. The fractional cross peak volume increase with mixing time was plotted for critical proton pairs and is shown in Figure 8A,B for ALDH1 and ALDH2, respectively. The intensities of cross peaks connecting H_N2 and H_N6 with the anomeric proton, H_N1', of the nicotinamide ribose ring were similar. This relationship was observed for both the mitochondrial and the cytosolic

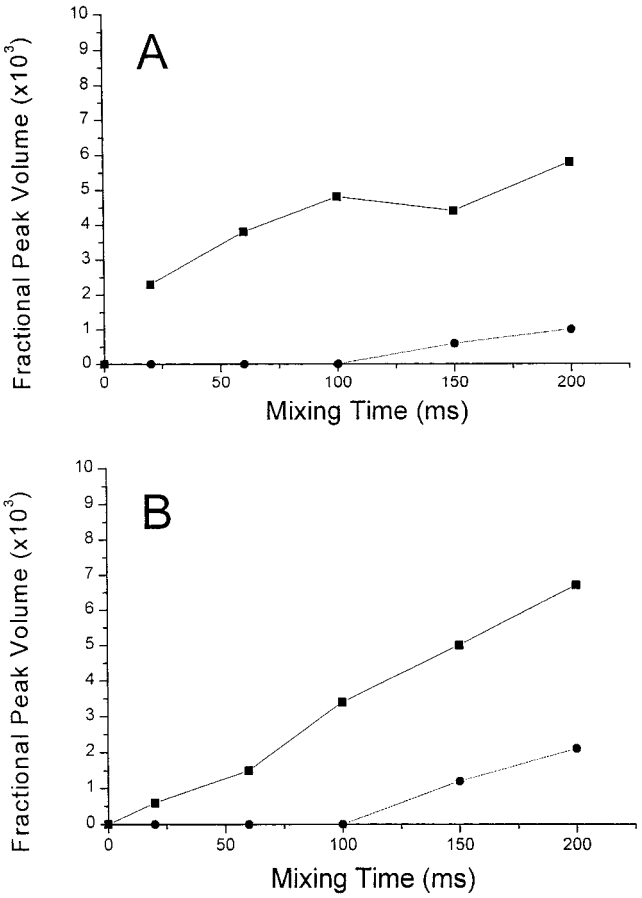

FIGURE 7: TrNOESY build-up curves for selected adenosine protons of 3 mM NAD bound to ca. 35 μM ALDH1 and ALDH2 at 20 °C. Integrated peak volumes, as a fraction of the auto-peak volume at $\tau_m = 20$ ms, are plotted versus mixing time for (A) ALDH1 + NAD and (B) ALDH2 + NAD. The cross peaks plotted are (■) H_A8-H_A1', (●) H_A2-H_A1'.

enzymes. Among other interactions, the most intense between nicotinamide and ribose rings were connecting H_N2 with H_N3'. This interaction was completely unexpected based on the crystal structure. The NMR data suggested several possible explanations. The ribose ring may have adopted a different conformation in solution than in the crystal, secondary NOE effects may have been occurring, or there was significant conformational mobility in the nicotinamide so that the similar cross peak intensities were the result of conformational averaging.

The state of NAD while bound to the E399Q mutant was examined using the transferred NOESY experiment. In this case, the H_A2-H_A1' interaction was more prominent than in experiments involving ALDH1, suggesting less specific binding of the adenine. The data revealed that the nicotinamide ring did not adopt a single, favored orientation relative to the ribose ring (Figure 9). The relationship between H_N2 and H_N6 with the ribose protons was nearly equivalent. The H_N2-H_N3' was no longer the largest but was similar in magnitude to the other interactions observed. The uniformity of cross peak magnitude is consistent with conformational averaging and together with the results of the saturation transfer experiments gives the image of increased conformational mobility of NAD when bound to the mutant. Data of this type are not appropriate for either distance or structure calculations because they would produce results correspond-

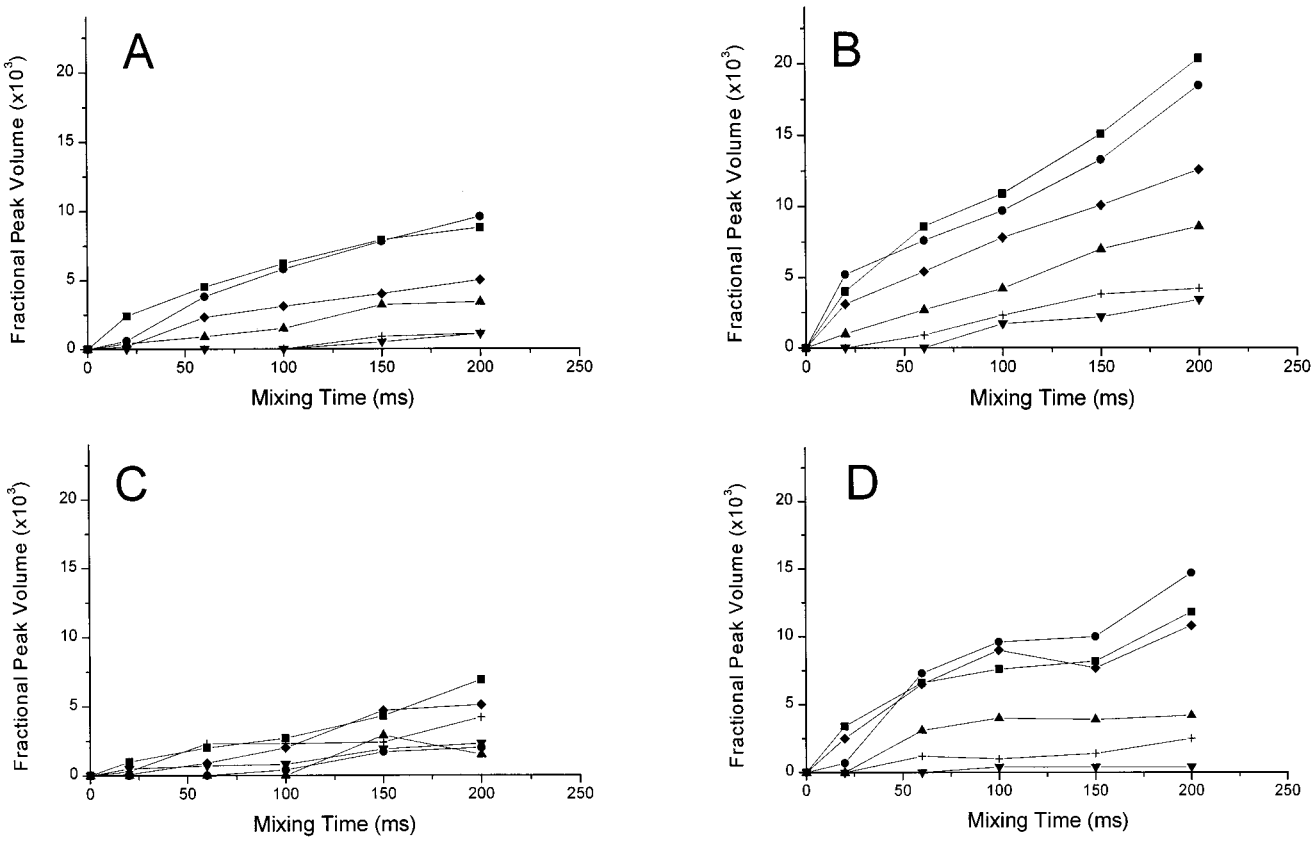

FIGURE 8: TrNOESY build-up curves for selected nicotinamide protons of 3 mM NAD bound to ca. 35 μM ALDH1 and ALDH2 in the absence and presence of Mg^{2+} ions at 20 °C. Integrated peak volumes, as a fraction of the auto-peak volume at $\tau_m = 20$ ms, are plotted versus mixing time for (A) ALDH1 + NAD, (B) ALDH2 + NAD, (C) ALDH1 + NAD + 10 mM Mg^{2+}, and (D) ALDH2 + NAD + 10 mM Mg^{2+}. The cross peaks plotted are (■) H_N2-H_N1', (●) H_N6-H_N1', (△) H_N2-H_N2', (▼) H_N6-H_N2', (◇) H_N2-H_N3', and (+) H_N6-H_N3'.

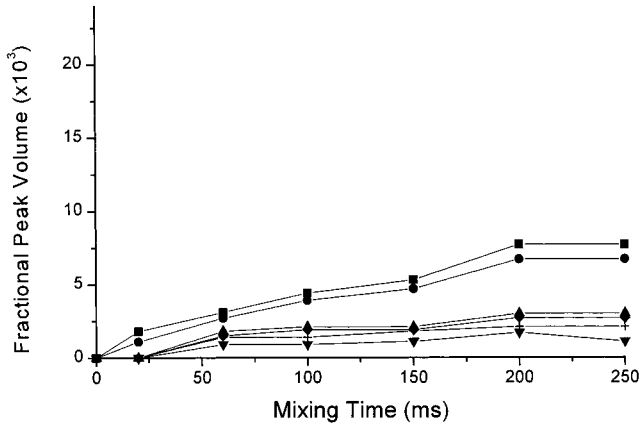

FIGURE 9: TrNOESY build-up curves for selected nicotinamide protons of 3 mM NAD bound to the E399Q mutant (ca. 35 μM) at 20 °C. Integrated peak volumes, as a fraction of the auto-peak volume at $\tau_m = 20$ ms, are plotted versus mixing time for E399Q + NAD. The cross peaks plotted are (■) H_N2-H_N1', (●) H_N6-H_N1', (△) H_N2-H_N2', (▼) H_N6-H_N2', (◇) H_N2-H_N3', and (+) H_N6-H_N3'.

ing to an average conformation and not one that is relevant to catalysis.

Conformational Preferences of NADH When Bound to ALDH. The conformation of NADH when bound to ALDH may be more useful than that of NAD for answering questions about catalysis. Although the rate-determining steps for catalysis by ALDH1 and ALDH2 differ, they both occur after NADH is formed (*23*−*25*). If differences were found in NADH conformation, it could help to explain why the rate-determining step of catalysis differs for the two isozymes. When bound to either ALDH1 or ALDH2, the adenine of NADH contained characteristics that were qualitatively similar to the adenine of NAD in the published structure (*3*). The H_A8-H_A2' interaction was the most prominent from this portion of the molecule (Figure 10). An interaction between H_A2 and H_A1' was observed only at long mixing times and the H_A8-H_A1' interaction did not appear at the shortest mixing times. The H_A8-H_A1' interaction ought to contain a significant contribution from a secondary NOE via the path $H_A8-H_A2'-H_A1'$ (Table 2). Predictions based on the distances obtained form the crystal structure would be expected to show a much greater difference between H_A8-H_A2' and H_A8-H_A1' than what was observed.

Relative cross peak intensities pertaining to the nicotinamide end of NADH were in stark contrast to those of NAD. The 2D spectra contain an obvious cross peak connecting H_N2 to H_N1' when NADH is bound to ALDH1. There was no similar cross peak connecting H_N6 with H_N1'. Only the nearby anti-phase cross peak arising from the *J* coupling (zero-quantum coherence) between H_N6 and H_N5 ($\delta = 4.76$ ppm) was observed. This cross peak may have obscured the H_N6-H_N1' ($\delta = 4.73$ ppm) interaction which was nonetheless much smaller in magnitude than H_N2-H_N1' (Figure 11). In addition, the interaction of H_N6 with H_N2' was the most intense interaction observed. When NADH was bound to ALDH2, the H_N2-H_N1' and H_N6-H_N2' interactions were the most intense, with H_N2-H_N1' clearly the largest. Again,

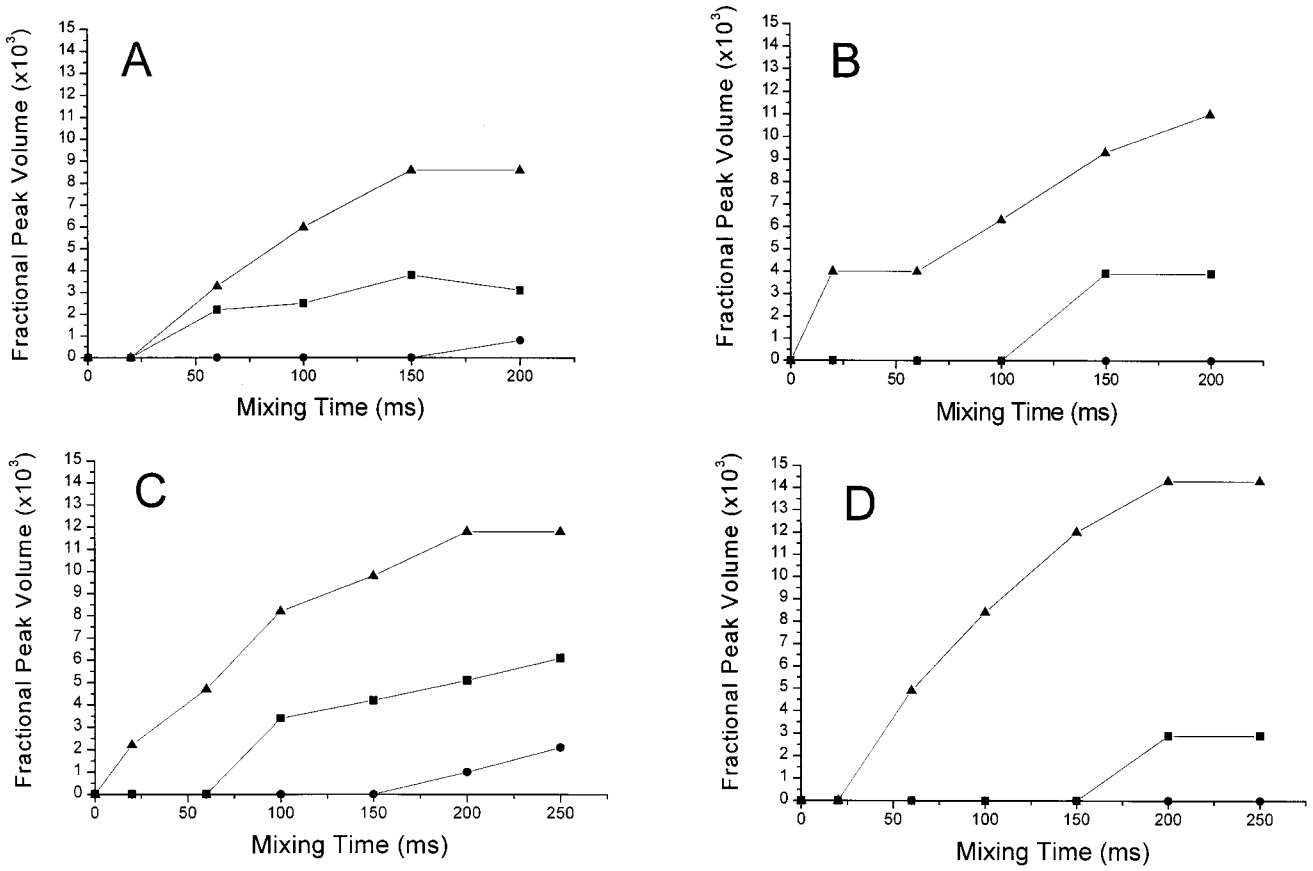

FIGURE 10: TrNOESY build-up curves for selected adenosine protons of 3 mM NADH bound to ca. 35 μM ALDH1 and ALDH2 in the absence and presence of Mg^{2+} ions at 20 °C. Integrated peak volumes, as a fraction of the auto-peak volume at $\tau_m = 20$ ms, are plotted versus mixing time for (A) ALDH1 + NADH, (B) ALDH2 + NADH, (C) ALDH1 + NADH + 10 mM Mg^{2+}, and (D) ALDH2 + NADH + 10 mM Mg^{2+}. The cross peaks plotted are (■) H_A8-H_A1', (●) H_A2-H_A1', (△) H_A8-H_A2'.

the H_N6-H_N1' interaction was much smaller than the H_N2-H_N1' interaction. While interactons between the aromatic protons and H_N3' were seen clearly in the ALDH−NAD spectra, they were not readily observed in spectra involving NADH ($\delta = 4.26$ ppm). Interaction between H_N2, H_N6 and H_N5',H_N5'' were observed in some of the ALDH−NADH spectra. These data are consistent with a population of NADH nicotinamide−ribose conformers dominated by the conformation of NAD as observed in the ALDH2 crystal structure. The interproton distances in the structure would suggest a far greater difference between H_N2-H_N1' and H_N6-H_N2' and the other interactions when compared to what was actually observed. Although the effects of conformational averaging appear to be reduced with NADH, the phenomenon must still have occurred. In addition, secondary NOEs may have also contributed to minimizing the difference between the interactions. Despite the leveling influence of conformational averaging and secondary NOEs, the data show in increase in the population of conformations in which the H_N2-H_N1' and H_N6-H_N2' interactions are large.

Affect of Magnesium Ions on Coenzyme Conformation. To assess the affect of Mg^{2+} ions on local nicotinamide conformation, transferred NOESYs were obtained in the presence of 10 mM Mg^{2+} ion. These data were compared to the data obtained without Mg^{2+} ions. A change in the relative intensities of interproton relationships was observed with NAD bound to ALDH1. Instead of a fairly broad range of values among the interactions that were monitored (Figure 8C), the peak volumes had greater similarity and were smaller in magnitude. The H_N2-H_N1' and H_N6-H_N1' proton interactions were no longer the most intense. The H_N6-H_N1' interaction was not visible in the 20 or 60 ms mixing time data, and when it was observed at longer mixing times it may have likely contained contributions from secondary Overhauser interactions. The change in relative magnitude of the H_N2-H_N1' and H_N6-H_N1' interactions suggests a Mg^{2+}-induced change in the conformational preferences of NAD. In contrast, the data from ALDH2 appeared very similar in the presence and absence of Mg^{2+} ions (Figure 8D).

In the data obtained for the complexes of NADH with ALDH1 and ALDH2 and 10 mM Mg^{2+} ions, the adenosine region approached the pattern predicted from the crystal structures. The H_A8-H_A2' interaction was, by far, the most intense (Figure 10C,D). The H_A8-H_A1' interaction was observed only at the longest mixing times used, and H_A2-H_A1' was not observed at all. The intensity disparity was most apparent with ALDH2. These results indicate that the adenosine portion of the molecule contained some conformational variability that was diminished when Mg^{2+} ions were present.

For the NADH−ALDH1 complex, the most intense interaction observed in the nicotinamide region was between H_N6 and H_N2'. In the presence of 10 mM Mg^{2+} ions, the H_N2-H_N1' and H_N6-H_N2' were of similar magnitude while H_N6-H_N1' was not observed. However, the differences were relatively small, suggesting that NADH was bound to ALDH1 with a preferred conformation and that the confor-

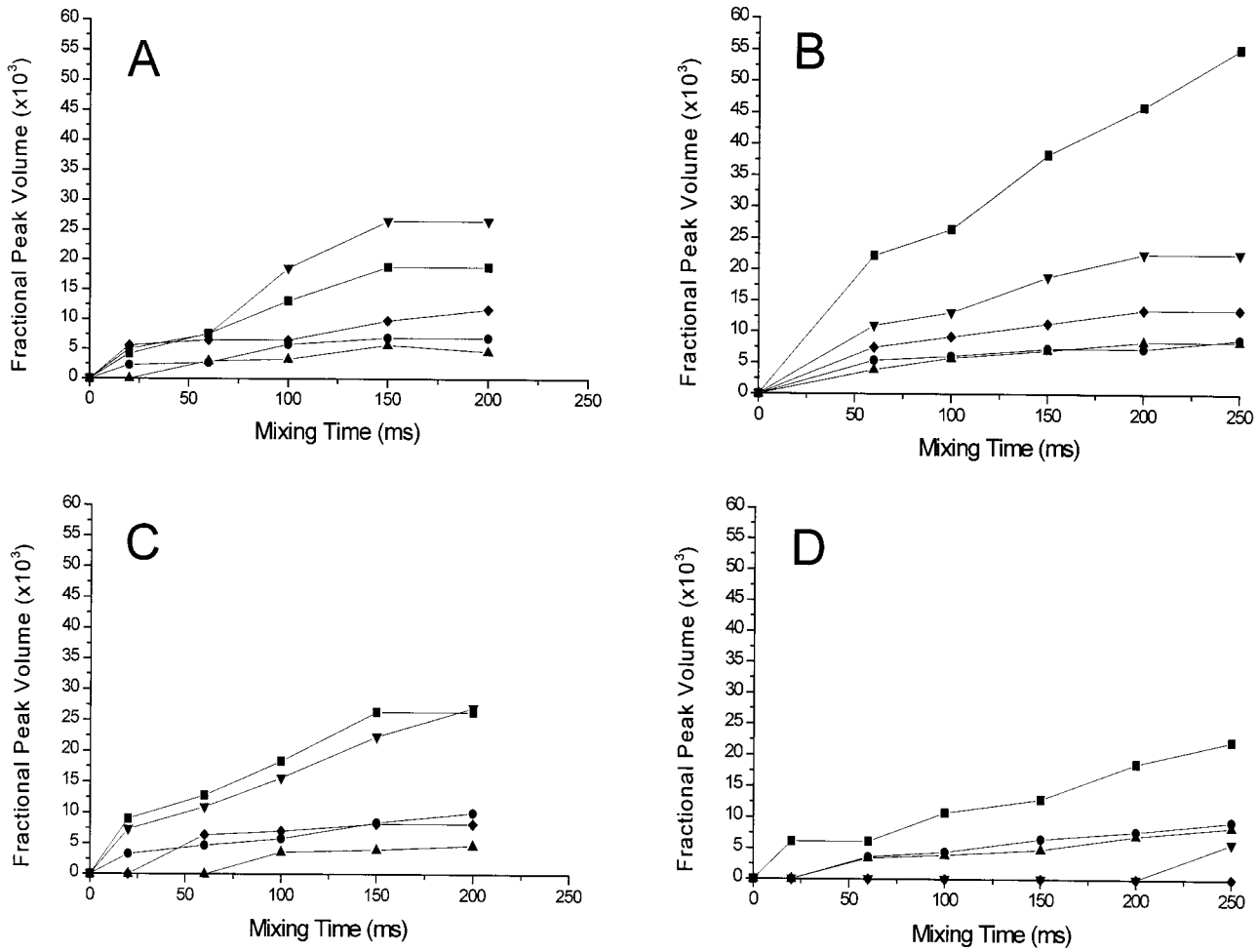

FIGURE 11: TrNOESY build-up curves for selected nicotinamide protons of 3 mM NADH bound to ca. 35 μM ALDH1 and ALDH2 at 20 °C. Integrated peak volumes, as a fraction of the auto-peak volume at $\tau_m = 20$ ms, are plotted versus mixing time for (A) ALDH1 + NADH, (B) ALDH2 + NADH, (C) ALDH1 + NADH + 10 mM Mg^{2+}, and (D) ALDH2 + NADH + 10 mM Mg^{2+}. The cross peaks plotted are (■) H_N2-H_N1', (●) H_N2-H_N2', (△) H_N2-H_N5', (▼) H_N6-H_N2', (◇) H_N6-H_N5'.

mational preferences of NADH were not altered significantly by the presence of the cation (Figure 11C). For NADH−ALDH2, the pattern of cross peak intensities was similar to that of ALDH1, including $H_N2-H_N1' \gg H_N6-H_N1'$ and $H_N2-H_N2' < H_N6-H_N2'$ (Figure 11D). When the metal cation was added, the pattern of intensities changed. The H_N6-H_N2' interaction was one of the most prominent in the absence of Mg^{2+} ions and virtually disappeared in the presence of the cation. The cross peak intensity pattern appeared to tend toward that which would be expected from the structure of NAD in complex with ALDH1 (*3*). These data reveal a cation-induced conformational change of NADH that could help to explain the activation of ALDH2 by magnesium.

DISCUSSION

STD Experiments. We wanted to learn if the solution methods could elucidate the conformational characteristics of the coenzyme, in both oxidized and reduced forms, and provide insight into how coenzyme conformation is involved in catalysis by ALDH. The crystallographic data show two NAD conformations that differ in the phosphodiester region and the orientation of the nicotinamide ring relative to its ribose (*2*, *3*). NMR data reveal that NAD maintains significant conformational heterogeneity while bound to either ALDH1 or ALDH2. It is likely that conformational changes occur via mobility of both the phosphodiester region and the nicotinamide.

ALDH has the apparent ability to bind NAD in what could be described as a population of conformations. STD experiments were employed to provide details of the interaction between ALDH and NAD. The STD experiment was initially used as a means of identifying the most promising ligands from a mixture (*16*, *17*). Subsequently, it has been utilized to identify the binding epitope of oligosaccharides to antibodies (*26*). With a similar purpose, we have analyzed the binding characteristics of specific ligands, NAD and NADH, and have observed differences in binding within the ligand. We have attempted to interpret the differences with respect to the published crystallographic data.

From the published structural data, distances between hydrogen-bearing atoms of NAD and the enzymes were determined. These distances are relevant to the STD experiment. The adenosine makes contact with essentially the same residues in ALDH1 and ALDH2. The atoms C_A2, C_A8, and C_A1' average nearly six contacts of less than 5 Å with hydrogen-bearing carbon atoms of the proteins. A greater amount of variation can be seen in the nicotinamide region. In the ALDH1 structure, the atoms C_N2, C_N4, C_N6, C_N1', and C_N2' average nearly eight contacts less than 5 Å, while

in the ALDH2 structure the average number of contacts is fewer than six. The most notable difference between the two enzymes is that the nicotinamide in the ALDH1 structure contains no atoms less than 5 Å from atoms of C302, while in the ALDH2 structure several nicotinamide atoms are within 5 Å of C302 atoms.

On the basis of the preceding analysis, the nicotinamide would be expected to exhibit evidence of greater interaction than the adenine with ALDH1. In contrast, the nicotinamide and adenine regions would be expected to interact to a similar extent with ALDH2. The observed STD data are, in general, contrary to these predictions. The adenine protons were saturated to a greater extent than those of the nicotinamide, and the protons of the nicotinamide were saturated uniformly. One explanation for the discrepancy is that the nicotinamide ring was highly mobile when bound. It has been demonstrated that motion with a relatively short rotational correlation time reduces the magnitude of NOEs (*27*, *28*). Saturation transfer operates under the same kinetic conditions as the NOE, so motion with a short rotational correlation time would be expected to reduce the extent of this phenomenon as well. If the nicotinamide protons sampled multiple environments during the time the molecule was bound, it would lead to the types of saturation transfer values that were observed.

Correspondence to X-ray Structural Data. The presence of metal cations in the crystallization solvent produced mixed effects on the ability to define electron density for the nicotinamide ring. In the presence of 0.2 mM $MgCl_2$, the nicotinamide was not observed with bovine ALDH2 but was observed in the heavy atom derivative containing 2 mM $SmCl_3$ (*2*). In each case, the cation was located near one of the adenine phosphate oxygens and appeared to stabilize particular phosphodiester rotamers via additional interactions with the nicotinamide phosphate oxygens. Sheep ALDH1 was crystallized in the presence of a relatively high concentration of $MgCl_2$ (170 mM). The Mg^{2+} ions were found near the phosphate oxygens (Moore, S., private communication). The structure contained a defined nicotinamide conformation (*3*), yet evidence appeared for multiple conformations of the NAD molecule. When human ALDH2 was crystallized in the presence of 8 mM Mn^{2+} ions and NAD, two tetramers were found together. Three subunits contained NAD in the conformation found in the ALDH2 structure with Sm^{3+} ions and five contained NAD in a conformation similar to that in ALDH1 (*29*). Apparently, a conformational mixture is possible within a single tetrameric enzyme assembly. The B-factors related to the coenzyme are high and variable, which certainly indicates atomic motion. Whether this reflects multiple discrete conformations or large atomic displacements due to vibrational events cannot be distinguished in the available data. Although no electron density was observed for alternative conformations within a single coenzyme binding site, it is not possible to rule out the occurrence of low populations of other conformations.

It can be seen from the comparison of ALDH1 and ALDH2 crystallographic data that conformational differences exist in the phosphodiester of NAD and the orientation of the nicotinamide ring to its ribose. The TrNOESY data of ALDH1 with NADH did not show evidence of a Mg^{2+} ion-dependent change in nicotinamide/ribose orientation. However, the FRET data revealed that Mg^{2+} ions brought about a change in the environment of the nicotinamide ring. The most likely interpretation of these data is that the FRET observations were mainly due to movement of the phosphodiester.

The presence of magnesium ions had a mixed effect on NMR data involving NAD as well. The STD experiments detect the interaction of ligand protons with those of the protein. No significant changes were observed as the Mg^{2+} ion concentration increased to 10 mM. The TrNOESY data detect the local conformational preferences of the ligand. The presence of Mg^{2+} ions appeared to have some effect on the orientation of the nicotinamide relative to the ribose when bound to ALDH1. The transferred NOEs indicated a shift in population toward the major conformation observed in the crystal structure of ALDH1. Conversely, in the presence of Mg^{2+} ions, only small changes were observed in the TrNOESY data of NAD when bound to ALDH2. From these data, we can formulate a model of NAD such that it is bound by the adenine but highly mobile in the nicotinamide region.

The most significant effects were observed in the conformational preferences of NADH. Both STD and TrNOESY data revealed that the reduced coenzyme had less mobility than NAD when bound to either enzyme. Both fluorescence and TrNOESY data indicated that the nicotinamide ring became reoriented when Mg^{2+} ions were added. The pattern of cross peak intensities in the TrNOESY data derived from NADH in complex with either enzyme would be expected if the population of the conformation of NAD in the ALDH2 structure had increased. With ALDH1, the STD experiments showed some differences in interaction with the enzyme, but the TrNOESY revealed no major changes in nicotinamide conformational preferences. With ALDH2 in the presence of Mg^{2+} ions, STD experiments detected no significant changes in interaction of NADH with the enzyme, but the cross peak intensity patterns shifted in the TrNOESY data. The NADH nicotinamide displayed a shift in conformational preference toward that observed in the structure of ALDH1.

Interpretation with Respect to Catalysis. In the time since the structures of ALDH1 and ALDH2 in complex with NAD were solved, it has been difficult to rationalize the position of the nicotinamide ring with respect to catalysis. The improper positioning of the nicotinamide ring for either hydride transfer or general base function, as shown by X-ray data, could be resolved if NAD was viewed as being highly mobile when bound to ALDH. The coenzyme binding site of ALDH is formed in a unique way by residues that do not anchor the nicotinamide. The NMR data reveal that the bound NAD molecule moves with relative freedom. While the nicotinamide is in a contracted position, like that seen in the ALDH1 structure, E268 should be able to abstract the proton from C302, thus activating the cysteine as a nucleophile. After nucleophilic attack on the substrate, NAD mobility should allow it to adopt a conformation capable of receiving the hydride from the ALDH−substrate adduct. If the NAD was too mobile or could not adopt the necessary conformation to receive a hydride ion, hydride transfer could become rate-limiting. It appears that the NAD was too mobile with the E399Q mutant, so the rate-limiting step changed to hydride transfer (*18*). The fluorescence anisotropy data we have presented indicate that Mg^{2+} ions have a much greater effect than substrate propanal on nicotinamide motion. Therefore, it does not appear that the conformational mobility

of the coenzyme attains greater restriction when this substrate is bound.

One aim of this study was to try to understand the effects of magnesium on the catalytic rates. Magnesium ions have an inhibitory effect on ALDH1 (*7*). The NMR data showed that Mg^{2+} ions further reduced the mobility of the nicotinamide but did not alter the local conformation. The FRET data indicate an environmental change in the presence of Mg^{2+} ions. From a thermodynamic perspective, catalytic rates depend on the free energy of both the ground and transition states. The loss in nicotinamide mobility with Mg^{2+} ions should reduce the entropy of the ALDH−NADH complex, thereby raising its free energy. We do not know the effect on the transition state, but the loss of mobility is mediated by Mg^{2+} ions that bind to the coenzyme phosphates. If the coenzyme binding site is not involved in restraining the conformational mobility of the nicotinamide, it can be estimated that the entropy effect on the transition state would be similar to or less than that of the ground state. Therefore, the rate effect of Mg^{2+} ions on ALDH1 must be based on the binding enthalpy of NADH. Fluorescence binding data show that the presence of Mg^{2+} ions enhances the binding of NADH to the enzyme (*30*). A mobile nicotinamide would be expected to form only transient hydrogen bonds or ionic interactions with complementary groups in the enzyme. The restriction of nicotinamide motion by Mg^{2+} ions would allow interactions with the enzyme to become more firmly established. Because the rate-limiting step of the reaction catalyzed by ALDH1 is NADH dissociation, the transition state probably involves the partial breaking of these interactions. Therefore, the enthalpy effect is likely to be greater in the ground state than in the transition state, leading to an increase in activation enthalpy in the presence of Mg^{2+} ions.

The influence of magnesium on the rate-determining step of catalysis by ALDH2 can be more fully understood from the data presented in this paper. Magnesium ions activate ALDH2 for which deacylation and release of the substrate is rate-limiting. For this step to occur, the general base, E268, must activate a water molecule that can make a nucleophilic attack on the enzyme−substrate adduct. The conformationally mobile coenzyme molecule will be able to sterically block this reaction step. Our data show that Mg^{2+} ions induce a change in the population of the local nicotinamide conformation of NADH. This would increase the proportion of time the conformation looks like the contracted phosphodiester of the ALDH1 structure. With the shift in population, E268 would no longer be blocked by the nicotinamide ring and could more freely play its role as general base in the deacylation reaction. As stated previously, the FRET data suggest that the conformational change involved movement of the phosphodiester as well as the nicotinamide. Therefore, such a conformational change would lead to a clear path for attack of an activated water molecule on the thioester.

Evidence for nicotinamide conformational averaging has been reported in studies of lactate dehydrogenase (*22*), malate dehydrogenase (*21*), and glutamate dehydrogenase (*20*). Binding of the coenzyme to lactate dehydrogenase induced a subtle conformational change in the protein that assisted the catalytic process (*31*). For ALDH2, a comparison of the apoenzyme and the enzyme in complex with NAD shows no evidence of a protein conformational change that supports the catalytic function of the enzyme (*32*). The data we have presented show that NAD binds to the enzyme such that the nicotinamide portion of the molecule samples a population of conformers. The binding of the coenzyme in this way may be the manner used by ALDH to solve the problem of how to bring the necessary catalytic functional groups together throughout the reaction cycle.

ACKNOWLEDGMENT

The authors thank Susan Carlson of Thomas Hurley's laboratory for her assistance with the large-scale preparations of ALDH1 and ALDH2.

REFERENCES

1. Liu, Z.-J., Sun, Y.-J., Rose, J., Chung, Y.-J., Hsiao, C.-D., Chang, W.-R., Kuo, I., Perozich, J., Lindahl, R., Hempel, J., and Wang, B.-C. (1997) *Nat. Struct. Biol. 4*, 317−326.
2. Steinmetz, C. G., Xie, P., Weiner, H., and Hurley, T. D. (1997) *Structure 5*, 701−711.
3. Moore, S. A., Baker, H. M., Blythe, T. J., Kitson, K. E., Kitson, T. M., and Baker, E. N. (1998) *Structure 6*, 1541−1551.
4. Farrés, J., Wang, T. T. Y., Cunningham, S. J., and Weiner, H. (1995) *Biochemistry 34*, 2592−2598.
5. Wang, X.-P., and Weiner, H. (1995) *Biochemistry 34*, 237−243.
6. Sheikh, S., Ni, L., Hurley, T. D., and Weiner, H. (1997) *J. Biol. Chem. 272*, 18817−18822.
7. Takahashi, K., Weiner, H., and Hu, J. H. (1980) *Arch. Biochem. Bipophys. 205*, 571−578.
8. Studier, F. W., and Moffat, B. A. (1986) *J. Mol. Biol. 189*, 113−130.
9. Zheng, C.-F., Wang, T. T. Y., and Weiner, H. (1993) *Alcohol.: Clin. Exp. Res. 17*, 828−831.
10. Sanger, F., Nicklen, S., and Coulson, A. R. (1977) *Proc. Natl. Acad. Sci. U.S.A. 74*, 5463−5467.
11. Ghenbot, G., and Weiner, H. (1992) *Protein Expression. Purif. 3*, 470−478.
12. Campbell, A. P., and Sykes, B. D. (1993) *Annu. Rev. Biophys. Biomol. Struct. 22*, 99−122.
13. Delaglio, F., Grzesiek, S., Vuister, G. W., Zhu, G., Pfeifer, J., and Bax, A. (1995) *J. Biomol. NMR 6*, 277−293.
14. Lakowicz, J. R. (1983) *Principles of Fluorescence Spectroscopy*, Plenum Press, New York.
15. Cordat, E., Mus-Veteau, I., and Leblanc, G. (1998) *J. Biol. Chem. 273*, 33198−33202.
16. Klein, J., Meinecke, R., Mayer, M., and Meyer, B. (1999) *J. Am. Chem. Soc. 121*, 5336−5337.
17. Mayer, M., and Meyer, B. (1999) *Angew. Chem., Int. Ed. 38*, 1784−1788.
18. Ni, L., Sheikh, S., and Weiner, H. (1997) *J. Biol. Chem. 272*, 18823−18826.
19. Jones, K. H., Lindahl, R., Baker, D. C., and Timkovich, R. (1987) *J. Biol. Chem. 262*, 10911−10913.
20. Banerjee, S., Levy, G. C., Limuti, C., Goldstein, B. M., and Bell, J. E. (1987) *Biochemistry 26*, 8443−8450.
21. Hall, M. D., and Banaszak, L. J. (1993) *J. Mol. Biol. 232*, 213−233.
22. Vincent, S. J. F., Zwahlen, C., Post, C. B., Burgner, J. W., and Bodenhausen, G. (1997) *Proc. Natl. Acad. Soc. U.S.A. 94*, 4383−4388.
23. Feldman, R. I., and Weiner, H. (1972) *J. Biol. Chem. 247*, 267−272.
24. Weiner, H., Hu, H. J. H., and Sanny, C. G. (1976) *J. Biol. Chem. 251*, 3853−3855.
25. Blackwell, L. F., Motion, R. L., MacGibbon, A. K., Hardman, M. J., and Buckley, P. D. (1987) *Biochem. J. 242*, 803−808.
26. Maaheimo, H., Kosma, P., Brade, L., Brade, H., and Peters, T. (2000) *Biochemistry 39*, 12778−12788.
27. Kumar, A., James, T. L., and Levy, G. C. (1992) *Isr. J. Chem. 32*, 257−261.

28. Nirmala, N. R., Lippens, G. M., and Hallenga, K. (1992) *J. Magn. Reson. 100*, 25−42.
29. Ni, L., Zhou, J., Hurley, T. D., and Weiner, H. (1999) *Protein Sci. 8*, 2784−2790.
30. Vallari, R. C., and Pietruszko, R. (1984) *J. Biol. Chem. 259*, 4927−4933.
31. Holbrook, J. J., Liljas, A., Steindel, S. J., and Rossmann, M. G. (1975) *The Enzymes* (Boyer, P. D., Ed.) 3rd ed., Academic Press, New York.
32. Hurley, T. D., Steinmetz, C. G., and Weiner, H. (1999) in *Enzymology and Molecular Biology of Carbonyl Metabolism 7* (Weiner, H., Maser, E., Crabb, D. W., and Lindahl, R., Eds.) pp 15−25, Plenum Publishers, New York.

BI012197T